2011

Detecting Specific Saccharides via a Single Indicator

Soojin Lim
Portland State University

Jorge O. Escobedo
Portland State University

Mark Lowry
Portland State University

Robert M. Strongin
Portland State University, strongin@pdx.edu

Published in final edited form as:
Chem Commun (Camb). 2011 August 7; 47(29): 8295–8297. doi:10.1039/c1cc11343g.

Detecting specific saccharides *via* a single indicator[†,‡]

Soojin Lim, **Jorge O. Escobedo**, **Mark Lowry**, and **Robert M. Strongin**
Department of Chemistry, Portland State University, Portland, Oregon 97207, USA.

Abstract

An improved synthesis of a rhodamine boronic acid indicator is reported. This compound is used in an optimized data collection protocol for wavelength- and time-dependent selectivity of sugars such as fructose and ribose derivatives. One indicator is thus used to selectively distinguish structurally related sugar analytes.

The development of simple optical indicators is of great current interest for the detection of small molecule disease biomarkers.[1] Selective detection is usually attributed to the distinctive interaction between the analyte and indicator or receptor. However, several indicator-biomolecule complexes may co-exist in a dynamic equilibrium. This is particularly relevant in complex natural sample matrices and wherein supramolecular or reversible covalent interactions are the basis of the analyte-selective signaling. Although the presence of a variety of indicator-bound species may hinder selective detection, the structural differences between the various complexes may afford distinctive absorption and emission profiles, thereby potentially allowing for multianalyte detection *via* a single optical indicator. Herein we propose that by judicious selection of specific excitation and emission wavelengths one may use a single indicator dye for the tunable detection of specific saccharides. The use of wavelength switching, rather than indicator or receptor structure changes, embodies a relatively streamlined approach to chemosensing.

In 2006 we published the first report of a boronic acid indicator (**1**) that was more selective for ribose, adenosine, nucleosides and nucleotides (including AICAr, the commercially available model succinylpurine metabolite for the rare autism spectrum disorder ADSL deficiency,[2] Fig. 1) as compared to fructose, the compound for which typical boronic acid compounds are inherently selective.[3] More recently, **1** has been used as a fluorescence turn-on probe to visualize specific tetraserine motifs in peptides and proteins in live cells.[4]

Probing the mechanism for attaining unique selectivity towards ribose and congeners using **1** as a platform has been of ongoing interest in our labs. This effort is in order to aid the design of indicators for specific nucleosides as well as thiol-derived biomarkers[5] of methylation status and oxidative stress (*e.g.,* SAM and SAH).[6] As part of the current study we report an improved preparation of **1** (Scheme 1) *via* a one-pot microwave-assisted synthesis. Conversion to **1** occurs with better yield (70%) and reaction time (20 min compared to > 24 h previously).[7] It is obtained *via* filtration of the product mixture rather than *via* the previously reported chromatographic methods (Scheme 1).

[†]This article is part of the ChemComm 'Supramolecular chemistry' web themed issue marking the International Year of Chemistry 2011.

[‡]Electronic supplementary information (ESI) available: Synthesis and characterization data of compound 1, additional spectral and computational data.

Correspondence to: Robert M. Strongin.
strongin@pdx.edu; Fax: +1 503-725-9525; Tel: +1 503-725-9724.

Typically, an excitation wavelength near the absorption maximum of a dye is selected for chemosensing. However, relying on the absorption maximum of an indicator in a buffer solution that does not contain analytes or potential interferences may not be optimal. For example, the optimum excitation wavelength for our recently developed fluorogenic α,β-unsaturated monoaldehyde-based sensor for biological thiols was found to be different than the maximum absorption.[5] Accordingly, we find that solutions of **1** containing various analytes, when monitored over time at several different excitation and emission wavelengths, affords us large multidimensional data sets specific for various analytes. A subset of this data is presented in Fig. 2. According to the contour plots of excitation-emission matrices (EEMs) obtained in the excitation range 470 to 620 nm and emission range from 520 to 690 nm, solutions of **1**, and **1** with various analytes, display patterns which are distinguishable for each analyte. There are differences in fluorescence intensity; however, there are also clearly different spectral signatures. For example, consistent with our previous observations of the selectivity of **1** toward ribose when excited at 565 nm,[3] Fig. 2 reveals a relatively higher emission response for the riboside AICAr and SAM as compared to fructose in the emission region near 600 nm when excited near 565 nm. We have shown previously that the small non-specific interference from fructose signal in this wavelength region can be removed *via* the addition of non-fluorescent boronic acid derivatives.[3] However, we were surprised to note that **1** responded to fructose in a different spectral region (emission at *ca.* 550 nm) when excited near 510 nm.

This observation makes the specific detection of fructose, in addition to ribose derivatives, possible with this probe. Data were collected as EEMs as a function of time. From this large multidimensional data set, spectra can be extracted at a specific times or the intensity at a specific wavelength monitored as a function of time. These data provide specific analyte dependent features such as the excitation and emission wavelengths resulting in the greatest signal and the time at which this signal occurs. For example, compound **1** responds to fructose in a different spectral region than ribose-derivatives, *i.e.* near 550 nm when excited at shorter wavelength near 510 nm in a time dependent manner with the peak increasing over time. When plotted as a function of time at an excitation wavelength of 510 nm, ribose derivative-**1** solutions do not exhibit a significant emission response in this region (see supporting information). Fig. 3 demonstrates that **1** displays an increased response toward both AICAr or fructose as a function of time and wavelength. It also shows the selectivity of **1** for SAM versus SAH. The ratio of SAM:SAH is frequently used as an indicator of cellular methylation potential.[6] Interestingly, SAM and SAH can be distinguished from AICAr by a wavelegnth shift of approximately 10 nm in both excitation and emssion (λ_{ex} = 560 nm, λ_{em} = 587.5 nm) as can be seen in the contour plots of these analytes in Fig. 2 and 3.

The most dramatic example of time and wavelength dependent detection in using a single indicator is shown in Fig. 4. It is constructed simply by scanning the EEM of each solution every 4 min for 1 h. One can visually distinguish each of the analyte-**1** solutions qualitatively (Fig. 4A). Initial results also indicate that the system will function in a more complex setting, *i.e.* when two analytes are present at the same time. As proof of concept, mixtures of two analytes (fructose and AICAr) were investigated. Sample mixtures enriched in either AICAr or fructose display signatures of both individual analytes but with features of the major analyte more dominant. Although the response is complicated, advanced data processing (*i.e.* chemometrics) should simplify interpretation. efforts to quantify mixtures are ongoing. Work is also ongoing to better understand the dynamic processes including supramolecular and reversible covalent interaction involved in these unique analyte dependent signals and their changes over time. Our previous studies attributed the selectivity of the compound **1** emission upon excitation at 565 nm to the fact that its ribose complex can exhibit tighter binding to the fluorophore as compared to the corresponding fructose and glucose complexes.[3] Simulations showed that this can occur *via* a charged hydrogen bond to

the carboxylate moiety of **1**. Favorable ion pairing interactions are thus likely responsible for the differences in the response of 1 toward the relatively positive SAM compared to SAH. Energy minimization studies afford an analogous explanation for the selectivity for AICAr over fructose (570 nm excitation, Fig. 3) that involves AICAr-**1** extended intramolecular interactions of the aminoimidazole carboxamide moeity with both, the carboxylate oxygen and the remaining free boronic acid (Fig. 5).

In conclusion, we have developed an improved synthesis of **1** *via* a microwave-assisted reductive amination and an optimal data collection method for wavelength-time dependent selectivity *via* EEMs. The results herein show that it is possible to use such data sets to develop strategies for allowing one indicator to be used to selectively distinguish structurally related sugar analytes.

Supplementary Material

Refer to Web version on PubMed Central for supplementary material.

Notes and references

1. Rusin, O.; Lim, S.; Strongin, RM. Case Studies of Chemosensors for Organic Molecules in Chemosensors: Principles, Strategies, and Applications. Wiley; 2011. in press
2. Jaeken J, Vandenberghe G. Lancet. 1984; 2:1058. [PubMed: 6150139]
3. Jiang S, Escobedo JO, Kim KK, Alpturk O, Samoei GK, Fakayode SO, Warner IM, Rusin O, Strongin RM. J. Am. Chem. Soc. 2006; 128:12221. [PubMed: 16967973]
4. Halo TL, Appelbaum J, Hobert EM, Balkin DM, Schepartz A. J. Am. Chem. Soc. 2009; 131:438. [PubMed: 19105691]
5. Lim S, Escobedo JO, Lowry M, Xu XY, Strongin R. Chem. Commun. 2010; 46:5707.
6. Chiang PK, Gordon RK, Tal J, Zeng GC, Doctor BP, Pardhasaradhi K, McCann PP. FASEB J. 1996; 10:471. [PubMed: 8647346]
7. Kim KK, Escobedo JO, St Luce NN, Rusin O, Wong D, Strongin RM. Org. Lett. 2003; 5:5007. [PubMed: 14682751]

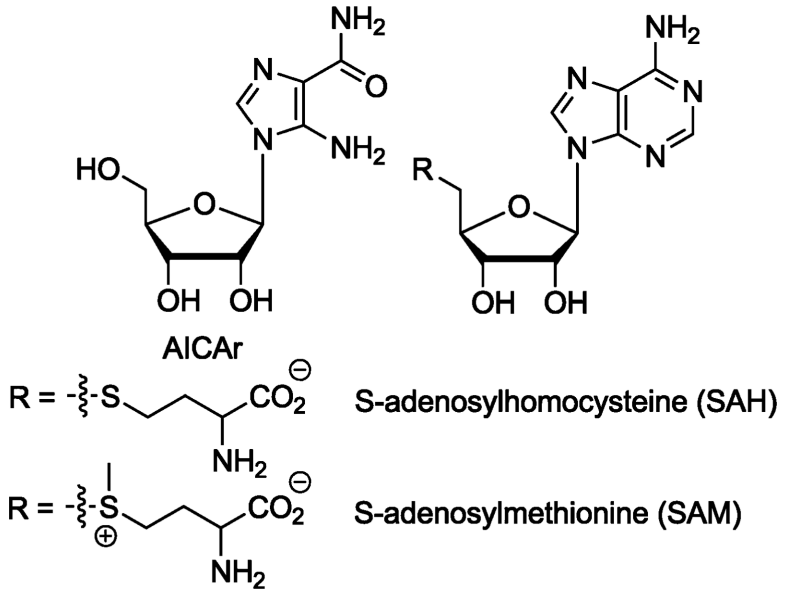

Fig. 1.
Ribose-containing molecules studied herein.

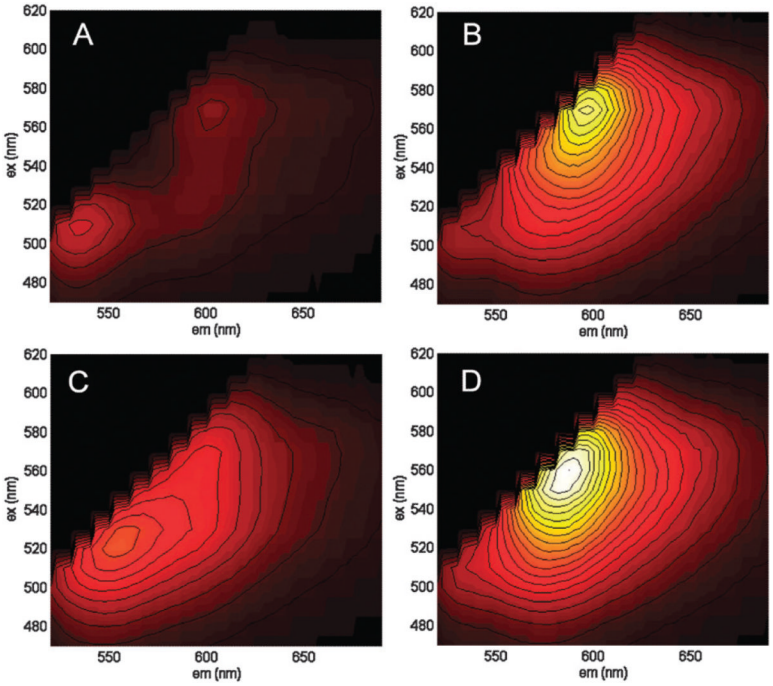

Fig. 2.

EEMs demonstrating the response of **1** towards various analytes. (A) **1** at 31 min, (B) **1** plus AICAr at 31 min, (C) **1** plus fructose at 58 min, and (D) **1** plus SAM at 11 min. The *x-axis* represents emission wavelength while the *y-axis* is excitation wavelength such that vertical and horizontal slices represent typical excitation and emission spectra respectively. Excitation and emission step sizes of 10 nm and 2.5 nm, respectively with a band pass of 5 nm for each. Fluorescence intensity is represented on the *z-axis* as various colors. Final concentration of **1** was 20 μM with each analyte at a concentration of 100 μM in 90% DMSO : 10% 25 μM pH 7.5 phosphate buffer. One part aqueous analyte was added to 9 parts **1** in DMSO followed by 15 s vortexing. EEMs were collected sequentially every 4 min for 1 h.

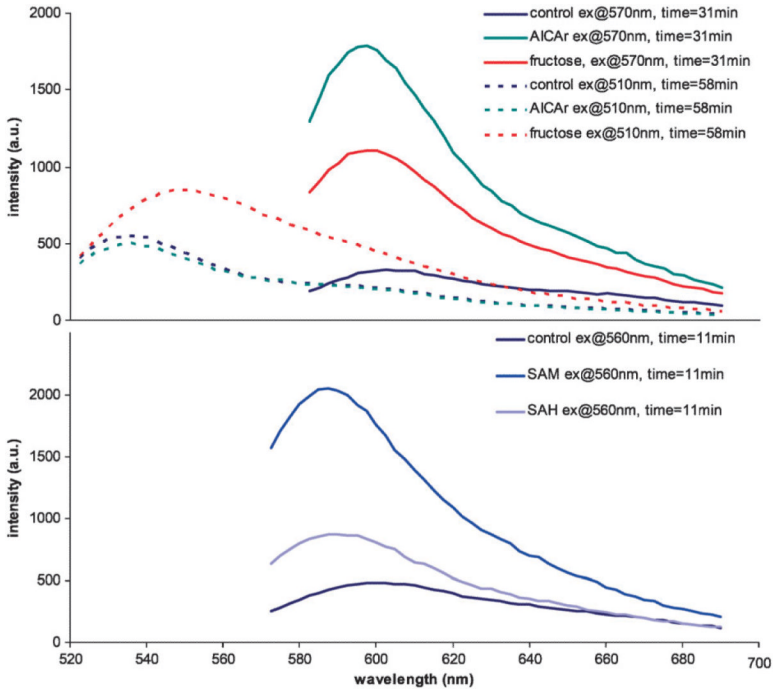

Fig. 3.

Emission spectra demonstrating selective response to various analytes. (Top) Control, AICAr and fructose emission spectra at given excitation wavelengths (510 or 570 nm) and times (31 or 58 min) after mixing. (Bottom) Control, SAM, and SAH emission spectra upon excitation at 560 nm and 11 min after mixing. Experimental conditions correspond to those described in Fig. 2.

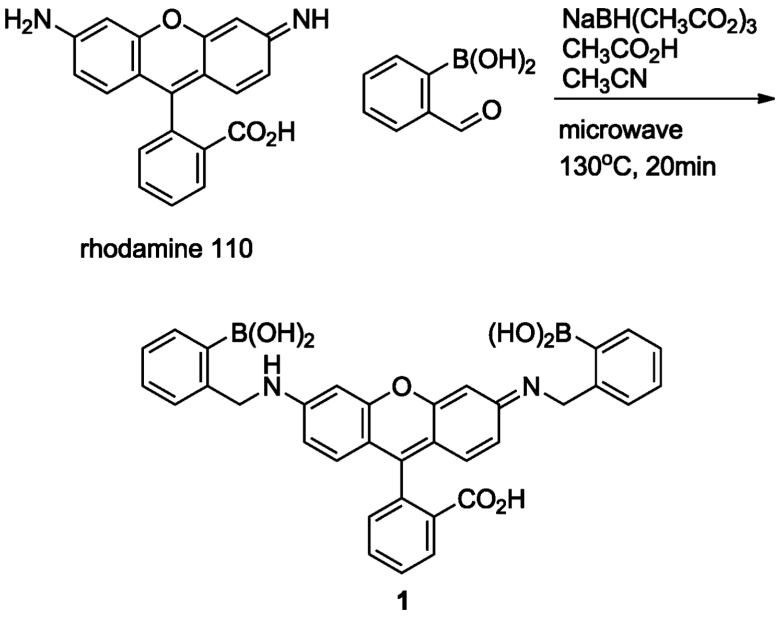

Scheme 1.
Microwave-assisted reaction of compound **1**.

Fig. 4.

Time and wavelength dependent detection. (A) EEMs of control and 1 plus 100 μM of analyte. (B) EEMs of 1 plus fructose and AICAr mixtures. Total concentration of each analyte mixture is 100 μM. The ratio of fructose to AICAr is increased toward the right as indicated. The first EEM in time is plotted at the bottom with time increasing toward the top. Experimental conditions as well as excitation and emission axes correspond to those in Fig. 2.

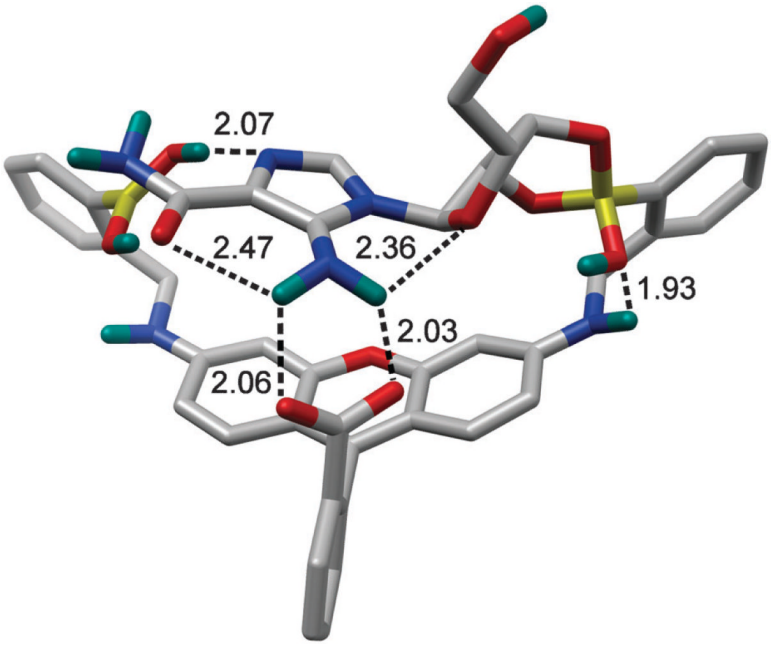

Fig. 5.
Energy-minimized model of the boronate ester formed after condensation of one equivalent of AICAr to **1**. Color atom codes: B = yellow, C = white, N = blue, O = red, H = cyan. Only hydrogen atoms involved in H-bond formation are displayed for simplicity. Dashed lines represent distance in angstroms.